

The Parton Branching Sudakov and its relation to CSS

A. Bermudez Martinez,^a F. Hautmann,^{a,b,c} L. Keersmaekers,^b A. Lelek,^{b,*} M. Mendizabal Morentin,^d S. Taheri Monfared^d and A.M. van Kampen^b

^a*CERN, Geneva, Switzerland*

^b*University of Antwerp, Belgium*

^c*University of Oxford, UK*

^d*Deutsches Elektronen-Synchrotron DESY, Germany*

E-mail: aleksandra.lelek@uantwerpen.be

The Transverse Momentum Dependent (TMD) Parton Branching (PB) method is a Monte Carlo (MC) approach to obtain QCD high energy collider predictions grounded in ideas originating from the TMD factorization. It provides an evolution equation for the TMD parton distribution functions (TMDs) and a framework to use those within TMD MC generators.

This work focuses on the structure of the PB Sudakov form factor. The Sudakov form factor is factorized in the perturbative and non-perturbative regions by introducing an intermediate separation scale motivated by angular ordering. The logarithmic order of the perturbative low- q_T resummation achieved so far by the PB Sudakov is discussed by comparing it to the Collins-Soper-Sterman (CSS) method and is increased up to next-to-next-to-leading logarithm (NNLL) with the use of physical (effective) coupling. A non-perturbative Sudakov form factor provides a term analogous to Collins-Soper (CS) kernel. The effects of different evolution scenarios, including or not the non-perturbative Sudakov contribution, on a numerical extraction of the CS kernel are investigated.

*The European Physical Society Conference on High Energy Physics (EPS-HEP2023)
21-25 August 2023
Hamburg, Germany*

*Speaker

1. Introduction

In the period of preparation for LHC High Luminosity phase and designing of new machines (e.g. Electron-Ion-Collider (EIC)) the need to develop general purpose Monte Carlo (MC) event generators becomes urgent. The baseline MC generators are based on collinear factorization [1] which assumes that partons move collinearly with the hadron they built and the transverse degrees of freedom are neglected. This limitation has to be however overcome and the 3D structure of hadrons has to be taken into account in order to exploit the full potential of the future experiments. The method, which was developed for this purpose, is the Transverse Momentum Dependent (TMD) Parton Branching (PB) [2, 3]: a MC framework to obtain QCD high energy collider predictions based on ideas originating from TMD factorization [4, 5]. In this work, the recent study of the PB Sudakov form factor in the context of TMD factorization [6] is summarized: the development to increase the precision of the PB TMD evolution equation to next-to-next-to-leading logarithm (NNLL) is presented and, in the second part of the paper, the Collins-Soper (CS) kernel extraction from PB predictions is performed, for different evolution scenarios.

2. PB Sudakov form factor

The TMD PB method provides an evolution equation [2, 3] for the momentum weighted TMD parton densities $x\mathcal{A}_a = \tilde{\mathcal{A}}_a$. Thanks to the momentum sum rule of the DGLAP splitting functions $\sum_b \int_0^1 dz z P_{ba} = 0$, the PB Sudakov form factor can be written with virtual splitting functions ¹

$$\Delta_a(\mu^2, \mu_0^2) = \exp\left(-\int_{\mu_0^2}^{\mu^2} \frac{d\mu'^2}{\mu'^2} \left(\int_0^{z_M} k_a(\alpha_s) \frac{1}{1-z} dz - d_a(\alpha_s)\right)\right), \quad (1)$$

where a is the parton species index, z is the splitting variable, z_M is the soft-gluon resolution scale, defining resolvable and non-resolvable branchings, μ' is the evolution variable defining the branching scale, and α_s is the strong coupling. PB applies angular ordering (AO) of Catani-Marchesini-Webber (CMW) [7], to relate the transverse momentum of the emitted parton q_\perp with the scale μ' and in most of the PB applications, the soft gluon resolution scale is $z_M \approx 1$. However, when one assumes the existence of a q_0 , a minimum q_\perp with which emitted parton can be resolved, then from AO one obtains a condition on maximum *dynamical* value of z_M [7]: $z_{\text{dyn}}(\mu') = 1 - q_0/\mu'$.

Motivated by AO, the PB Sudakov form factor of Eq. 1 with $z_M \approx 1$, can be decomposed in two regions by using as an intermediate scale z_{dyn} . With that, the phase space is divided in two regions: (i) perturbative (P) for $z < z_{\text{dyn}}$, which corresponds to $|q_\perp| > q_0$ and (ii) non-perturbative (NP) $z_{\text{dyn}} < z < z_M$ ($z_M = 1 - \epsilon$ with $0 \simeq \epsilon \ll 1$), for which $|q_\perp| < q_0$, resulting in

$$\begin{aligned} \Delta_a(\mu^2, \mu_0^2) &= \exp\left(-\int_{\mu_0^2}^{\mu^2} \frac{d\mu'^2}{\mu'^2} \left[\int_0^{z_{\text{dyn}}(\mu')} dz \frac{k_a(\alpha_s)}{1-z} - d_a(\alpha_s)\right]\right) \\ &\times \exp\left(-\int_{\mu_0^2}^{\mu^2} \frac{d\mu'^2}{\mu'^2} \int_{z_{\text{dyn}}(\mu')}^{z_M} dz \frac{k_a(\alpha_s)}{1-z}\right) = \Delta_a^{(P)}(\mu^2, \mu_0^2, q_0) \cdot \Delta_a^{(NP)}(\mu^2, \mu_0^2, \epsilon, q_0^2). \end{aligned} \quad (2)$$

¹The splitting functions can be decomposed as $P_{ab}(z, \alpha_s) = \delta_{ab} d_a(\alpha_s) \delta(1-z) + \delta_{ab} k_a(\alpha_s) \frac{1}{(1-z)_+} + R_{ab}(z, \alpha_s)$, with real parts being $P_{ab}^R = \delta_{ab} k_a(\alpha_s) \frac{1}{1-z} + R_{ab}(z, \alpha_s)$ and the virtual corrections $P_a^V = k_a \frac{1}{1-z} - d_a \delta(1-z)$.

This trick allows to discuss the resummation accuracy of PB and its non-perturbative component from the evolution.

Perturbative Sudakov: After mapping the evolution variable μ^2 to transverse momentum q_\perp^2 [8], assuming $\mu_0 \approx q_0 = \mathcal{O}(1 \text{ GeV})$ and using q_\perp^2 as the scale of α_s (as used commonly in PB applications), the perturbative Sudakov can be written as:

$$\Delta_a^{(P)}(\mu^2, q_0^2) = \exp\left(-\int_{q_0^2}^{\mu^2} \frac{dq_\perp^2}{q_\perp^2} \left[\frac{1}{2}k_a(\alpha_s) \ln\left(\frac{\mu^2}{q_\perp^2}\right) - d_a(\alpha_s)\right]\right). \quad (3)$$

The structure of Eq. 3 may be compared with the structure of the perturbative CSS Sudakov form factor which (with appropriate scale choices) can be written as

$$\Delta_a^{\text{CSS1 (P)}}(\mu^2, \mu_{b^*}^2) = \exp\left(-\int_{\mu_{b^*}^2}^{\mu^2} \frac{d\mu'^2}{\mu'^2} \left[A_a(\alpha_s) \ln\left(\frac{\mu^2}{\mu'^2}\right) + B_a(\alpha_s)\right]\right), \quad (4)$$

with A and B having the expansions $\mathcal{R}_a = \sum_n (\alpha_s/2\pi)^n \mathcal{R}_a^{(n)}$. One can then attempt to compare the PB and CSS coefficients order by order. A pure n^{th} logarithmic order cannot be obtained with Eq. 3. When leading order (LO) splitting functions are used, the $k_a^{(0)}$ coefficient coincides with $A_a^{(1)}$ providing the double logarithmic term at leading logarithmic (LL) accuracy and the $d_a^{(0)}$ coefficient coincides with $-\frac{1}{2}B_a^{(1)}$ giving the single logarithmic term at the next-to-leading logarithmic (NLL) accuracy. With next-to-leading order (NLO) splitting functions, the $k_a^{(1)}$ (equal to $A_a^{(2)}$) provides the double logarithmic term at NLL and a part of NNLL resummation is included by the $d_a^{(1)}$ coefficient. At this stage the pattern breaks: because of collinear anomaly [9] the NNLL resummation cannot be achieved by Eq. 3. The possible difference between the $d_a^{(1)}$ and $B_a^{(2)}$ of the PB and CSS can be explained by scheme dependence originating from the renormalization group equation [10] but the $A_a^{(3)}$ is scheme independent and the next-to-next-to-leading order (NNLO) DGLAP coefficient $k_a^{(2)}$ does not correspond to the CSS double logarithmic coefficient at NNLL, $A_a^{(3)}$.

Eq. 3 can be modified by introducing the physical (effective) soft-gluon coupling [7, 11, 12] to achieve NNLL:

$$\Delta_a^{(P)}(\mu^2, q_0^2) = \exp\left(-\int_{q_0^2}^{\mu^2} \frac{dq_\perp^2}{q_\perp^2} \left[\frac{1}{2}k_a(\alpha_s^{\text{phys}}) \ln\left(\frac{\mu^2}{q_\perp^2}\right) - d_a(\alpha_s^{\text{phys}})\right]\right), \quad (5)$$

where the physical soft-gluon coupling is defined as $\alpha_s^{\text{phys}} = \alpha_s \left(1 + \sum_{n=1}^{\infty} \mathcal{K}^{(n)} \left(\frac{\alpha_s}{2\pi}\right)^n\right)$. With a proper combination of DGLAP splitting functions at a given order and physical coupling with selected coefficients, the PB predictions with a pure NLL and NNLL coefficients in the Sudakov form factor are obtained for the first time [6]. In the left and middle panel of Fig. 1 one can see TMDs and integrated TMDs (iTMDs) for down quark at 100 GeV (and $x = 0.001$ for the TMD case) for the following evolution settings: 1.) NLO: NLO splitting functions + 2-loop α_s ; 2.) NLL: LO splitting functions + 2-loop α_s modified according to $\alpha_s^{\text{NLL}} = \alpha_s \left(1 + \mathcal{K}^{(1)} \left(\frac{\alpha_s}{2\pi}\right)\right)$; 3.) NNLL: NLO splitting functions + 2-loop α_s modified according to $\alpha_s^{\text{NNLL}} = \alpha_s \left(1 + \mathcal{K}^{(2)} \left(\frac{\alpha_s}{2\pi}\right)^2\right)$.

²The $\frac{1}{2}$ difference originates from the fact that in PB two separately evolved TMDs are matched with a matrix element to get the final cross section. In CSS notation, the exponents from the evolution of each TMD are combined in one common Sudakov form factor Δ_a^{CSS} .

In all curves, $z_M = 1 - 10^{-5}$ and $\alpha_s(q_\perp^2)$ is used and the starting distribution is HERAPDF2.0 [13]. The q_0 is chosen to be $q_0 = 1.0$ GeV, for $|q_\perp| < 1.0$ GeV α_s is frozen to the value $\alpha_s(q_0)$. The physical coupling has been implemented both in the Sudakov form factor as well as in the real emission probabilities to ensure momentum conservation [14]. Both for TMDs and iTMDs, the difference between NLL and NLO is significant whereas the difference between the NLO and NNLL predictions is of the order of few %. The investigated TMDs were matched by CASCADE3 [15] to NLO matrix element generated with iTMD PB-NLO-2018-Set2 [16] using the method of [17], to investigate the impact of NLL and NNLL evolution on Z boson p_\perp spectrum at LHC. From the right panel of Fig. 1 one can see that there is a large difference between the NLL and NLO results and the effect of going from NLO to NNLL is of the order of few %. The qualitative observed behaviour is similar to the results obtained e.g. in [18].

Non-perturbative Sudakov: In the region $|q_\perp| < q_0$, the argument of α_s is set to $\alpha_s(q_0)$. With that, the non-perturbative PB Sudakov is

$$\ln \Delta_a^{(\text{NP})}(\mu^2, \mu_0^2, \epsilon, q_0^2) = -\frac{k_a(\alpha_s)}{2} \ln\left(\frac{\mu^2}{\mu_0^2}\right) \ln\left(\frac{q_0^2}{\epsilon^2 \mu_0 \mu}\right). \quad (6)$$

The logarithm of μ^2/μ_0^2 corresponds to the CS kernel structure of the CSS method.

Motivated by this observation, we use the method of [19] to extract CS kernels from 4 phenomenological models, with and without Δ_a^{NP} , all evolved with NLO splitting functions and 2-loop α_s (i.e. no A_3 coefficient included): 1.) with $\alpha_s(q_\perp^2)$ and $z_M = 1 - 10^{-5}$, with $q_0 = 1.0$ GeV, $\alpha_s = \alpha_s(\max(q_0^2, q_\perp^2))$; 2.) with $\alpha_s(\mu'^2)$ and $z_M = 1 - 10^{-5}$; 3.) with $\alpha_s(q_\perp^2)$ and $z_M = 1 - q_0/\mu'$ with $q_0 = 1.0$ GeV (i.e. no non-perturbative Sudakov form factor); 4.) with $\alpha_s(q_\perp^2)$ and $z_M = 1 - q_0/\mu'$ with $q_0 = 0.5$ GeV (i.e. no non-perturbative Sudakov form factor). Obtained CS kernels are shown in Fig. 2. The results show sensitivity to the treatment of radiation: the model with the biggest amount of soft radiation (1.) is linear at large b . When the soft region is limited by neglecting the non-perturbative sudakov (3.), the kernel behaviour becomes flat at large b . When the q_0 is lowered to $q_0 = 0.5$ GeV (4.), the additional branchings compared to model 3. lead to a significant change in the large b region: despite having no non-perturbative Sudakov, the orange curve is close to the red one. The model with $\alpha_s(\mu')$ (2.) has a contribution from very soft radiation but different scale of the coupling leads to very different kernel shape.

3. Conclusions

The structure of the PB Sudakov form factor was investigated in the context of TMD factorization thanks to the decomposition of the PB Sudakov form factor into perturbative and non-perturbative parts, achieved by introducing an intermediate scale z_{dyn} motivated by AO. Using the physical soft-gluon coupling, the accuracy of the perturbative low q_\perp resummation of the PB Sudakov was extended up to NNLL. The non-perturbative Sudakov form factor revealed a structure of CS kernel. The CS kernel was extracted from PB predictions for 4 models, with and without non-perturbative Sudakov. Modelling of the radiation has a huge impact on the shape of extracted kernels.

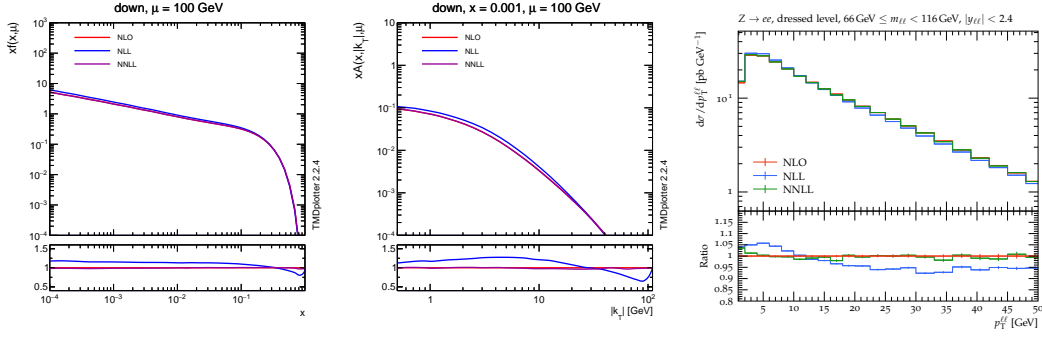


Figure 1: The PB iTMDs (left) and TMDs (middle) obtained with NLO, NLL and NNLL evolution for down quark at 100 GeV (and $x = 0.001$ for the TMD case). The prediction for Z boson p_{\perp} at 8 TeV (right) obtained with NLO ME matched to the TMDs shown in the middle plot.

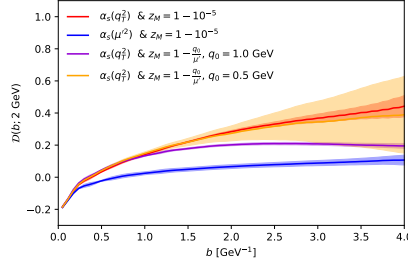


Figure 2: The CS kernels extracted from PB method for different evolution scenarios.

Acknowledgements A. Lelek acknowledges funding by Research Foundation-Flanders (FWO) (1272421N).

References

[1] J. C. Collins, D. E. Soper and G. F. Sterman, *Adv. Ser. Direct. High Energy Phys.* **5** (1989), 1-91 doi:10.1142/9789814503266_0001 [arXiv:hep-ph/0409313 [hep-ph]].

[2] F. Hautmann, H. Jung, A. Lelek, V. Radescu and R. Zlebcik, *Phys. Lett. B* **772** (2017), 446-451 doi:10.1016/j.physletb.2017.07.005 [arXiv:1704.01757 [hep-ph]].

[3] F. Hautmann, H. Jung, A. Lelek, V. Radescu and R. Zlebcik, *JHEP* **01** (2018), 070 doi:10.1007/JHEP01(2018)070 [arXiv:1708.03279 [hep-ph]].

[4] J. C. Collins, D. E. Soper and G. F. Sterman, *Nucl. Phys. B* **250** (1985), 199-224 doi:10.1016/0550-3213(85)90479-1

[5] J. Collins, *Camb. Monogr. Part. Phys. Nucl. Phys. Cosmol.* **32** (2011), 1-624 Cambridge University Press, 2013, ISBN 978-1-00-940184-5 doi:10.1017/9781009401845

[6] A. Bermudez Martinez, F. Hautmann, L. Keersmaekers, A. Lelek, M. Mendizabal Morentin, S. Taheri Monfared and A.M. van Kampen in preparation

- [7] S. Catani, B. R. Webber and G. Marchesini, Nucl. Phys. B **349** (1991), 635-654 doi:10.1016/0550-3213(91)90390-J
- [8] F. Hautmann, L. Keersmaekers, A. Lelek and A. M. Van Kampen, Nucl. Phys. B **949** (2019), 114795 doi:10.1016/j.nuclphysb.2019.114795 [arXiv:1908.08524 [hep-ph]].
- [9] T. Becher and M. Neubert, Eur. Phys. J. C **71** (2011), 1665 doi:10.1140/epjc/s10052-011-1665-7 [arXiv:1007.4005 [hep-ph]].
- [10] S. Catani, D. de Florian and M. Grazzini, Nucl. Phys. B **596** (2001), 299-312 doi:10.1016/S0550-3213(00)00617-9 [arXiv:hep-ph/0008184 [hep-ph]].
- [11] S. Catani, D. De Florian and M. Grazzini, Eur. Phys. J. C **79** (2019) no.8, 685 doi:10.1140/epjc/s10052-019-7174-9 [arXiv:1904.10365 [hep-ph]].
- [12] A. Banfi, B. K. El-Menoufi and P. F. Monni, JHEP **01** (2019), 083 doi:10.1007/JHEP01(2019)083 [arXiv:1807.11487 [hep-ph]].
- [13] H. Abramowicz *et al.* [H1 and ZEUS], Eur. Phys. J. C **75** (2015) no.12, 580 doi:10.1140/epjc/s10052-015-3710-4 [arXiv:1506.06042 [hep-ex]].
- [14] F. Hautmann, M. Hentschinski, L. Keersmaekers, A. Kusina, K. Kutak and A. Lelek, Phys. Lett. B **833** (2022), 137276 doi:10.1016/j.physletb.2022.137276 [arXiv:2205.15873 [hep-ph]].
- [15] S. Baranov *et al.* [CASCADE], Eur. Phys. J. C **81** (2021) no.5, 425 doi:10.1140/epjc/s10052-021-09203-8 [arXiv:2101.10221 [hep-ph]].
- [16] A. Bermudez Martinez, P. Connor, H. Jung, A. Lelek, R. Žlebčík, F. Hautmann and V. Radescu, Phys. Rev. D **99** (2019) no.7, 074008 doi:10.1103/PhysRevD.99.074008 [arXiv:1804.11152 [hep-ph]].
- [17] A. Bermudez Martinez, P. Connor, D. Dominguez Damiani, L. I. Estevez Banos, F. Hautmann, H. Jung, J. Lidrych, M. Schmitz, S. Taheri Monfared and Q. Wang, *et al.* Phys. Rev. D **100** (2019) no.7, 074027 doi:10.1103/PhysRevD.100.074027 [arXiv:1906.00919 [hep-ph]].
- [18] S. Camarda, L. Cieri and G. Ferrera, Phys. Rev. D **104** (2021) no.11, L111503 doi:10.1103/PhysRevD.104.L111503 [arXiv:2103.04974 [hep-ph]].
- [19] A. Bermudez Martinez and A. Vladimirov, Phys. Rev. D **106** (2022) no.9, L091501 doi:10.1103/PhysRevD.106.L091501 [arXiv:2206.01105 [hep-ph]].